

2. Dyke, S. F., Floyd, A. J., Sainsbury, M. and Theobald, R. S., *Organic Spectroscopy*, Penguin, 1971, pp. 74, 76.
3. Rao, C. N. R., *Chemical Applications of Infra-red Spectroscopy*, Academic Press, 1963, p. 193.
4. Jackman, L. M. and Sternhell, S., *Applications of Nuclear Magnetic Resonance Spectroscopy in Organic Chemistry*, Pergamon, 1969, pp. 164, 179, 189, 216.
5. Vogel, A. I., *Practical Organic Chemistry*, Longmans Green, 3rd edn., 1957, p. 187.
6. Seshadri, T. R. and Rangaswami, S., *Proc. Indian Acad. Sci.*, 1942, 15, 417.

## A MAGNETIC SURVEY ON CHARNOCKITES IN THE VICINITY OF VISAKHAPATNAM

### Introduction

A VERTICAL magnetometric survey is carried out on an area of 2.2 square furlongs in the vicinity of Visakhapatnam to trace the extension of some of the outcropping charnockite bands. The area is situated about 15 miles NNE of Visakhapatnam and is shown in Fig. 1. The topography of the area is characterised by a small hillock of 50 ft elevation ENE of the area and another of 15 ft. elevation WNW with outcropping khondalites. Charnockites have a higher intensity of magnetisation compared with the country rocks, khondalites. The higher intensity of magnetisation helps in tracing their presence and extent.

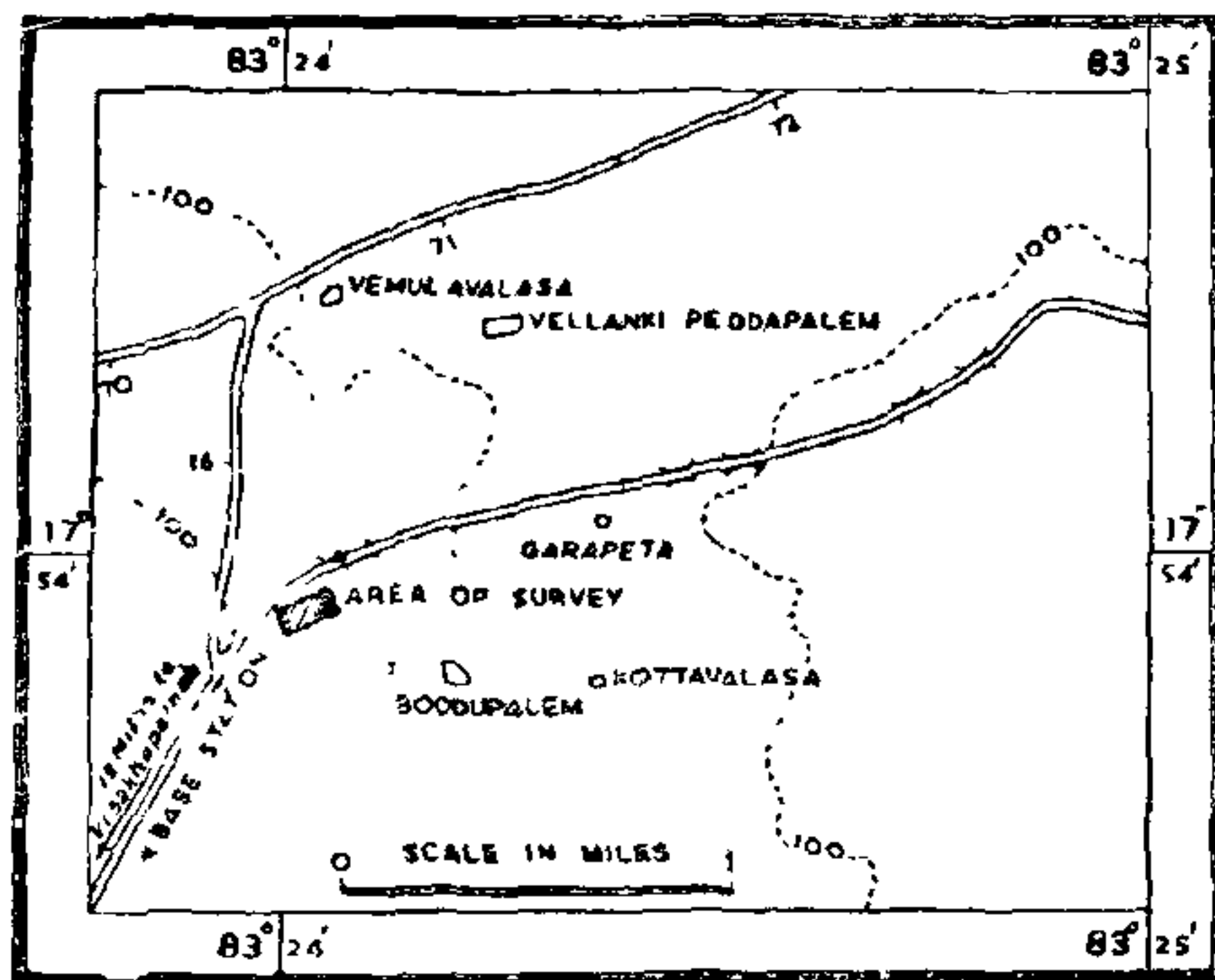


FIG. 1. Location map.

### Geology of the Area

The geology of the area is closely connected with the general geology of Eastern Ghats, which constitute mostly khondalites and intervening charnockites. The khondalite series is represented by garnet sillimanite gneisses, garnet-biotite-sillimanite gneisses and quartzites and the charnockite series by leptynites,

charnockites, granites and pegmatites. The khondalite series strike NW-SE with steep dips towards SW. The sillimanite gneisses and quartzites are interbedded. The banding in the charnockite series is parallel to that of the surrounding khondalites. The basic members of the charnockite series are black to gray in colour, hard and compact and medium to coarse grained. The members of the charnockite series are intimately associated with each other and occur together.

### Magnetic Survey

A vertical magnetometric survey is carried out with a Gf6 Schmidt-type Askania vertical magnetic field balance having a scale value of 92 gammas. The area is covered with 540 magnetic observations at intervals of 20 feet along lines separated from each other by 100 ft. The profile lines are laid along the direction N 45° E. The observations are corrected for diurnal variation of the vertical component of the geomagnetic field by observations made at intervals of 15 minutes at a magnetically undisturbed Base Station situated half-a-mile outside the area of survey. The vertical magnetic anomalies are shown contoured in Fig. 2.

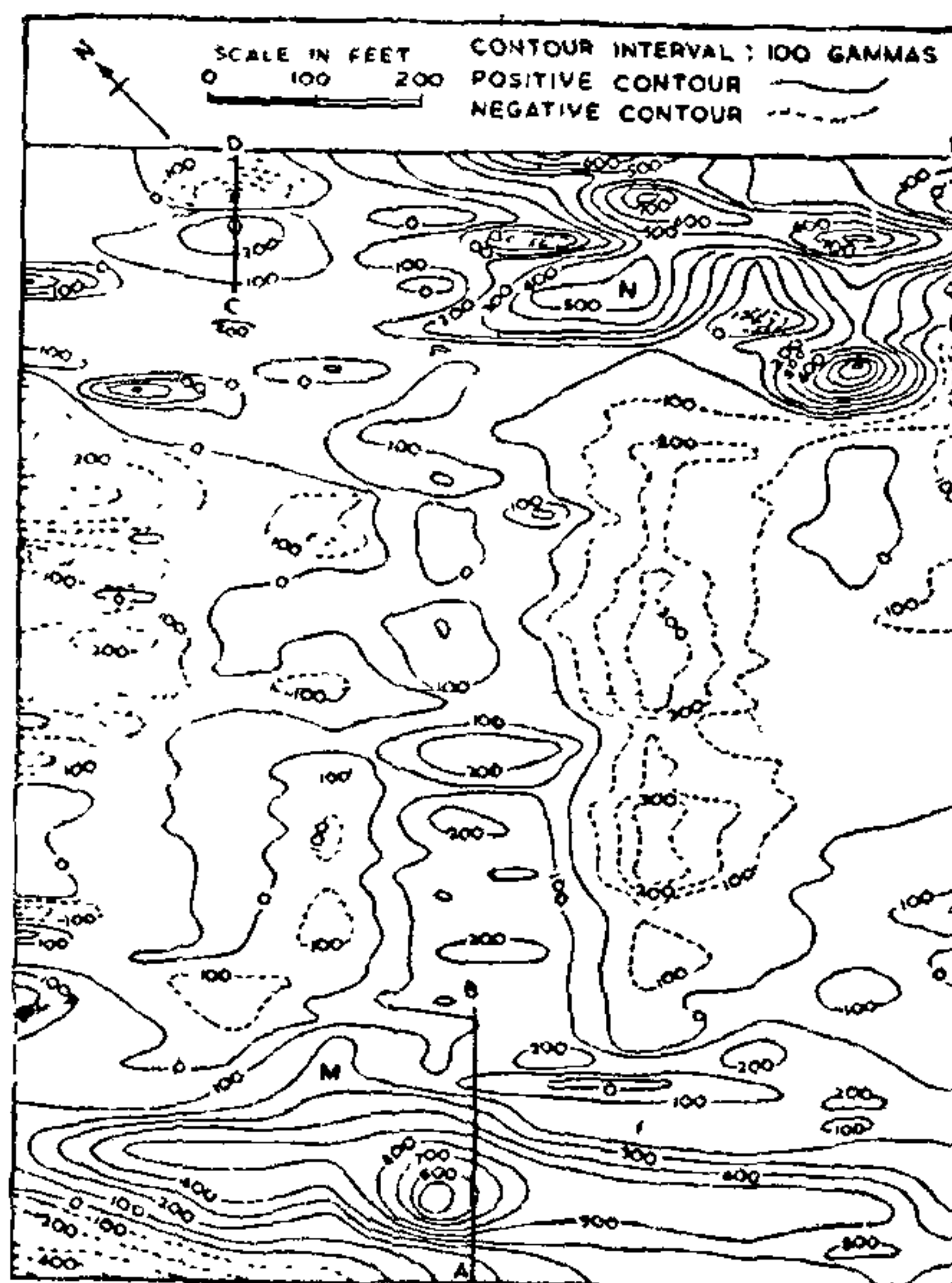


FIG. 2. Vertical magnetic anomaly map.

### Results and Interpretation

The magnetic anomalies range from -400 gammas to 1000 gammas with the major portion of the area

covered by positive anomalies. Two major anomaly distributions, one in the West-South-West in the region marked 'M' on the map and the other East-North-East in the region marked 'N' on the map, are observed. The anomalies in the region 'M' exhibit a regular elongated almost parallel pattern of contours indicating the possible extension of the causative body in the direction of the contours as also a fairly uniform magnetic polarisation and a possible continuity in depth. The contour distribution in the region 'N' is less regular with a number of small closures of steep gradients being observed. But the closures are aligned in a direction parallel to that of the pattern at 'M'. It seems that a clear trend is obviated by the effects of local weathering. This trend may also be indicating the extension of the causative body parallel to that at 'M'. Three profiles namely AB, CD and EF (Figs. 3-5), one-AB-across the pattern at 'M' and two-CD, EF across the pattern at 'N', are analysed quantitatively.

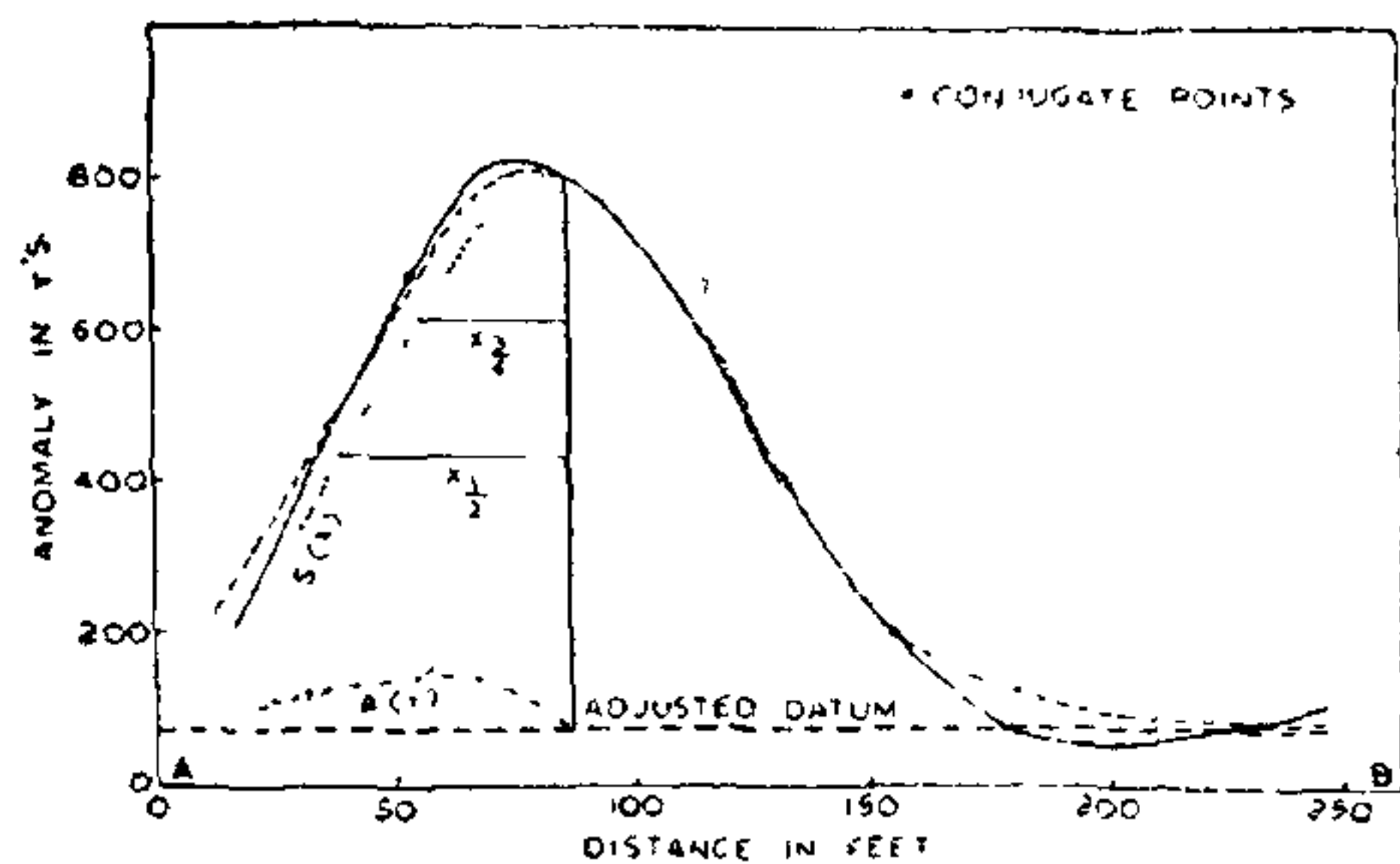


FIG. 3. Profile AB.

Because of the resemblance of the contour pattern to a two-dimensional anomaly and of the profile to a typical dyke anomaly, the profile AB (Fig. 3) is interpreted on an assumed dyke model by the method of Koulomzine *et al.*<sup>1</sup>. As outlined in the method the origin 'O' of the anomaly curve is found, the datum level is adjusted and the anomaly curve is split into symmetric,  $S(x)$ , and antisymmetric,  $A(x)$ , components (Fig. 3). As the antisymmetric component has very small amplitude the interpretation is carried out by using information from the symmetric component curve. The ratio,  $x_{1/2}/x_{3/4}$  (where  $x_{1/2}$  and  $x_{3/4}$  are the half widths at half and three-fourths the maximum amplitude) is used along with the three master curves (Koulomzine *et al.*<sup>1</sup>, p. 825) to obtain the values of depth ( $h$ ), width ( $w$ ), and the angle ( $Q$ ) made by the direction of magnetisation with the dyke in the plane of the profile. The values thus obtained are:  $h = 29.3$  ft,  $w = 73.7$  ft, and  $Q = 9^\circ$ . A dyke anomaly curve is calculated using these values and the curve is shown in Fig. 3 as a discontinuous line which shows the agreement between the two curves.

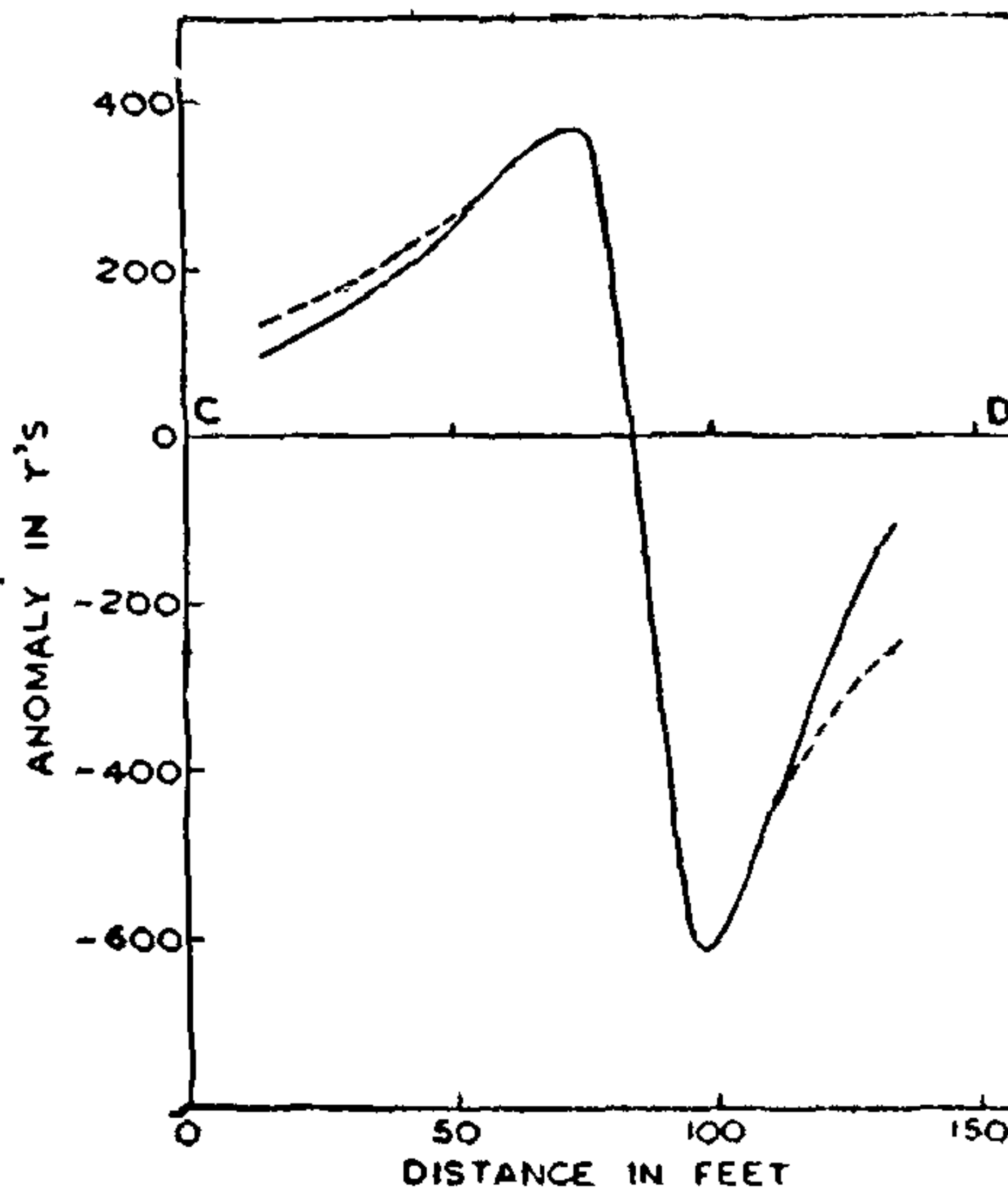


FIG. 4. Profile CD.

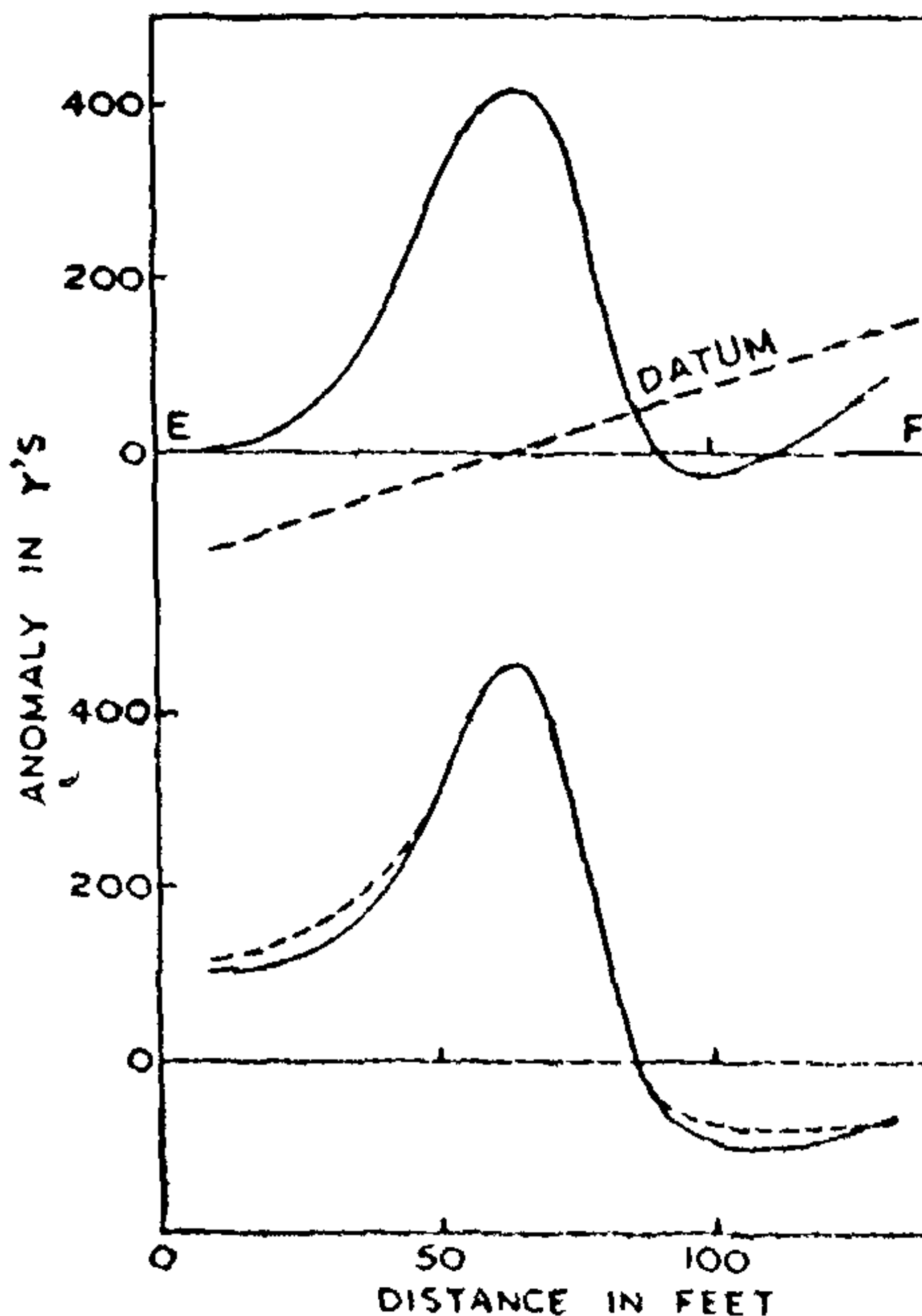


FIG. 5. Profile EF.

Since the pattern at 'N' also shows a trend parallel to that at 'M', a two-dimensional body is assumed as the source. The causative body is approximated to a thin dyke. The two profiles, CD and EF, are so chosen that the influence of adjoining anomalies is least on them. For the profile EF, the datum, as shown in Fig. 5, is chosen as indicated by the full length profile. The two profiles are interpreted by using the following rules<sup>2</sup>:

$$\frac{w_{1/2}}{h} = 2 \sec Q \quad (1)$$

$$\frac{w_{1/2}}{L} = \tan Q \quad (2)$$

where  $w_{1/2}$  is the half width of the anomaly curve and L is the horizontal distance between the maximum and minimum anomaly points. For the profile CD (Fig. 4), using the above rules, a depth of 18 ft and an angle Q of 153° are obtained. A theoretical anomaly curve is calculated and the values are changed until the theoretical curve agrees with the observed anomaly curve. Finally the values,  $h = 12.6$  ft. and  $Q = 105^\circ$ , are adopted and the corresponding theoretical curve is shown as a discontinuous curve in Fig. 4.

For the profile EF (Fig. 5) a depth of 15.7 ft. and a Q of 44° are obtained. The theoretical curve corresponding to the values obtained, which agrees well with the observed anomaly curve, is shown in the figure as a discontinuous line. The results of interpretation for all the profiles are presented in Table I.

TABLE I  
Results of interpretation

Profile	$h$ (feet)	$w$ (feet)	$Q^\circ$
AB	29.3	73.7	9
CD	12.6	..	105
EF	15.7	..	44

The charnockite body is observed in a road cut and followed with magnetic observations. The anomaly trends at 'M' and 'N' in the magnetic anomaly map are the expressions of subsurface extensions of the charnockite bands. The magnetic anomaly patterns at 'M' and 'N' indicate that the magnetic polarisation in the charnockite band at 'M' is more uniform than in the other at 'N'. The depths obtained and presented in Table I indicate that the two charnockite bands are at a shallow depth. The band at 'N' has a smaller width than that at 'M'. The angles of magnetisation, Q, obtained for the profiles CD and EF reflect

the changes in the direction of magnetisation, from one point to another along the strike of the band.

Department of Geophysics, V. BHASKARA RAO.  
Andhra University, Waltair, A. LAKSHMIPATI RAJU.  
December 7, 1977.

1. Koulomzine, *et al.*, *Geophysics*, 1970, 35, 812.
2. Grant, F. S. and West, G. F., *Interpretation Theory in Applied Geophysics*, (McGraw-Hill Book Co.), 1965, p. 326.

#### CYTOKININ-LIKE BEHAVIOUR OF SOME B VITAMINS IN *BOUGAINVILLEA* *SPECTABILIS* WILLD., AND GREEN GRAM (*PHASEOLUS RADIATUS* L.)

No comprehensive investigation is carried out on the role of B vitamins on plant growth. Galston<sup>1</sup> has pointed out that nicotinic acid and IAA in the dark, favour root initiation while in the light these reagents favour shoot growth. Thus, there appears to be similarity in action of growth substances and vitamins. The present study has been designed to get more information in their action and to assign them the function of growth substances.

Leaf discs of *Bougainvillea spectabilis* were soaked in 10 and 20 PPM of cytokinin, riboflavin and pantothenic acid in dark. Seeds of green gram var. Cultivar were subjected to presowing soaking in 10 and 20 PPM solutions of riboflavin and pantothenic acid for 24 h, after which they were allowed to grow in distilled water for 8 days in petridishes in a luminosity of 2,000 Lux. The vitamin treatment was given in darkness as the vitamin B<sub>2</sub> is light sensitive. The protein and the chlorophyll were estimated according to the methods of Lowry *et al.*,<sup>2</sup> and Arnon *et al.*,<sup>3</sup> respectively. Pantothenic acid (10 PPM) appears to retard senescence by decreasing the rate of chlorophyll breakdown in the dark (Table I). On the fifth day, the decrease in chlorophyll content in the control was from 0.286 to 0.196 mg while in pantothenic acid (10 PPM) treated leaf discs, it was from 0.275 to 0.214 mg (0.061 mg). The decrease with 20 PPM pantothenic acid was from 0.306 to 0.219 mg (0.087 mg). With riboflavin (20 PPM), the control of chlorophyll breakdown was more effective on the third day as compared with the fifth day (Table I). Cytokinin (kinetin) at 20 PPM was more effective than at 10 PPM in controlling chlorophyll breakdown (control = 0.096, kinetin 20 PPM = 0.064, kinetin 10 PPM = 0.082 mg decrease respectively on the fifth day when the fifth day value is subtracted from the second day value). Thus, it appears that pantothenic acid at 10 PPM was more effective than cytokinin at 10 PPM. Riboflavin was effective only at 20 PPM and at the initial state (third day only)